

ROBUST AND SCALABLE LEARNING OF DATA MANIFOLDS WITH COMPLEX TOPOLOGIES VIA ELPIGRAPH

Luca Albergante^{1,2,3}, Evgeny M. Mirkes^{4,5}, Huidong Chen^{6,7,8}, Alexis Martin^{1,2,3}, Louis Faure^{1,2,3,9}, Emmanuel Barillot^{1,2,3}, Luca Pinello^{6,10}, Alexander N. Gorban^{4,5}, Andrei Zinovyev^{1,2,3}

¹ Institut Curie, PSL Research University, F-75005 Paris, France

² INSERM, U900, F-75005 Paris, France

³ MINES ParisTech, PSL Research University, CBIO-Centre for Computational Biology, F-75006 Paris, France

⁴ Department of Mathematics, University of Leicester, University Road, Leicester LE1 7RH, UK

⁵ Lobachevsky University, Nizhni Novgorod, Russia

⁶ Molecular Pathology Unit & Cancer Center, Massachusetts General Hospital and Harvard Medical School, Boston, MA 02114, USA

⁷ Department of Biostatistics and Computational Biology, Dana-Farber Cancer Institute and Harvard T.H. Chan School of Public Health, Boston, MA 02215, USA

⁸ Department of Computer Science and Technology, Tongji University, Shanghai 201804, China

⁹ Institute of Technology and Innovation (ITI), PSL Research University, PSL Research University, F-75005 Paris, France

¹⁰ Broad Institute of MIT and Harvard, Cambridge, MA 02142, USA

The correspondence should be sent to Andrei.Zinovyev@curie.fr or Luca.Albergante@curie.fr.

Abstract

We present *ELPiGraph*, a method for approximating data distributions having non-trivial topological features such as the existence of excluded regions or branching structures. Unlike many existing methods, *ELPiGraph* is not based on the construction of a k -nearest neighbour graph, a procedure that can perform poorly in the case of multidimensional and noisy data. Instead, *ELPiGraph* constructs elastic principal graphs in a more robust way by minimizing elastic energy, applying graph grammars and explicitly controlling topological complexity. Using trimmed approximation error function makes *ELPiGraph* extremely robust to the presence of background noise without decreasing computational performance and allows it to deal with complex cases of manifold learning (for example, *ELPiGraph* can learn disconnected intersecting manifolds). Thanks to the quasi-quadratic nature of the elastic function, *ELPiGraph* performs almost as fast as a simple k -means clustering and, therefore, is much more scalable than alternative methods, and can work on large datasets containing millions of high dimensional points on a personal computer. The excellent performance of the method opens the possibility to apply resampling and to approximate complex data structures via *principal graph ensembles* which can be used to construct *consensus principal graphs*. *ELPiGraph* is currently implemented in five programming languages and accompanied by a graphical user interface, which makes it a versatile tool to deal with complex data in various fields from molecular biology, where it can be used to infer pseudo-time trajectories from single-cell RNASeq, to astronomy, where it can be used to approximate complex structures in the distribution of galaxies.

Introduction

Large datasets are becoming increasingly common in various fields of science. These datasets are frequently characterized by complex structures of multidimensional data clouds, difficult to appreciate by simple data visualization methods. To better characterize and quantify such structures, it is important to develop computational

methods aimed at providing a low complexity data representation, while preserving some essential features of the multidimensional data distribution.

When considering data distributions in high-dimensional spaces, two diametrically opposed scenarios need to be kept in mind^{1,2}. In some cases, clouds of data points can be located in a vicinity of a relatively low-dimensional object (such as principal manifold), and hence possess a *low intrinsic dimensionality*. Under these circumstances, numerous dimensionality reduction approaches, often used as part of machine learning pipelines in many scientific fields, can be efficient in recovering the low-dimensional object, either explicitly or implicitly and in projecting the data points onto it. This is the case of high extrinsic but low intrinsic dimensionality, where an informative low dimensional data projection exists. However, some clouds of data points are characterized by a truly high-dimensional structure. In this case, mathematical phenomena such as concentration of measures start to play an important role, and dimensionality reduction methods can become inadequate³. Nonetheless, such *curse of dimensionality* can also be a *blessing*, and approaches based on self-averaging or on the application of stochastic separability theory can be very successful^{4,5}. Notably, distinguishing the first situation from the second is an important scientific problem, which is not completely solved yet.

Manifold learning methods aim at modelling the multidimensional data as a noisy sample from an underlying generating manifold, usually of relatively small dimension. A classical linear manifold learning method is Principal Component Analysis (PCA) introduced more than 100 years ago⁶. From the 90s, multiple generalizations of PCA to non-linear manifolds have been suggested, including Self-Organizing Maps (SOMs)⁷, ISOMAP⁸, Local Linear Embedding (LLE)⁹, tSNE¹⁰, regularized principal curves and manifolds^{11–13} and many others¹⁴.

This paper is primarily focused on a particular case of non-linear manifold learning, where the true intrinsic structure of a dataset can be thought of as a one-dimensional continuum which, unlike simple principal curves, can possess a complex topology (e.g., branching points and closed paths). As often the case, it is convenient to represent the continuous data manifold in a certain number of points and map its topology onto a graph, which connects these points. Hence, we aim at reconstructing principal graphs which, by definition, are data approximations by graph embedding “passing through the middle of data” and possessing specific regular properties, which restrict the graph complexity^{15,16}.

High demand of appropriate methods for principal graph reconstruction has emerged recently in connection with novel sequencing technologies in molecular biology which are able to generate high-dimensional datasets characterized by an increased level of geometrical complexity. For example, clouds of data points representing heterogeneity of transcriptomic profiles of thousands of single cells are frequently characterized by curvilinear and branching structures. These structures reflect continuous changes in the regulatory programs and bifurcations of these programs during complex cell fate decisions (see Figure 4). The existence and biological relevance of such branching trajectories was clearly demonstrated while studying development¹⁷, cellular differentiation^{18–20} and cancer biology²¹. The power of such analyses stimulated the emergence of a number of tools for reconstructing so called “cellular trajectories” and “branching pseudotime” in the field of bioinformatics^{22–24}. Some of these tools exploit the notion of principal curves or graphs explicitly^{25,26}, while others sometimes use a different terminology closely related to principal graphs or principal trees in their purpose^{27,28}. Biology is, however, only one of the possible domains of applicability of principal graphs. They can serve useful data approximations in other fields of science such as political sciences or image processing^{13,29}.

Most of the methods currently used to learn complex non-linear data manifolds are based on the employment of an auxiliary object called k -nearest neighbour (k NN) graph, constructed by connecting each data point to its k closest (in a chosen metrics) neighbouring points (Figure 1B). To avoid unnecessary complexity, the k NN graph can be constructed using pre-clustered data distribution or a sample of the data. A popular mathematical tool for extracting the approximator graph structure from the k NN graph is the Minimal Spanning Tree (MST) or computationally feasible heuristics for its estimation. Despite its popularity, using MST or similar approaches can limit the ability of a method to discover only tree-like data approximators (i.e., principal trees). For example, if background noise is present or the underlying manifold spans many dimensions in the data space, the structure of the k NN graph, together with the reconstructed MST, can easily become very complex, non-robust and even misleading (see Figure 1B). In practice, the majority of the methods used for extracting branching data structures require drastic dimension reduction (to 3D or 2D), as the properties of k NN graph are more stable and tractable in such low dimensional spaces. However, it is easy to imagine toy examples describing, for example, a tree-like manifold embedded in a multi-dimensional space, containing intersecting branches in any linear 2D projection. Projecting in 3D should make exact intersection of manifold branches not typical: nevertheless, branches might easily appear much closer, after projection into lower dimension, than they are in higher dimensions and effectively intersect (especially when a manifold is sampled with noise). Moreover, most of the methods described in the literature rely on heuristics for estimating the optimal graph structure (such as the MST, for the tree-like topologies) and do not explore sufficiently large volume of the structural space to determine which approximating graph topology best describes the data.

In this paper we present a method for constructing elastic principal graphs together with its algorithmic implementation which we named EIPiGraph. The EIPiGraph method does not employ the notion of k NN graph, MST, or data pre-clustering. Moreover, it does not require data preprocessing via drastic dimensionality reduction. The method is almost as fast as standard k -means clustering for fitting a fixed graph structure to the data. This speed allows us to use it for exploring many graph topologies and find the optimal one by a gradient descent-like approach, driven by the application of graph grammars, in the space of graph structures. Moreover, EIPiGraph has a built-in resampling features that can be used to explore the robustness of the reconstructed structure to find a *consensus principal graph* for data approximation. Furthermore, EIPiGraph can be made extremely robust with respect to the presence of background noise, without affecting its computational performance. Moreover, in certain situations EIPiGraph allows dealing with self-intersecting data distributions, a situation too difficult for most of the existing methods.

EIPiGraph is built using previously introduced concepts (elastic energy functional, graph grammars)^{12,30,31}. However, the existing prototype implementation did not scale well, so the algorithm for optimization of graph embedment was recently designed de-novo, based on introducing the elastic matrix and Laplacian-based penalty (see Methods section). This allowed us to scale the performance of the algorithm to millions of points in relatively high (~ 100) dimensions, which arguably makes EIPiGraph the fastest currently available method for finding and fitting complex graph topology to data. A number of important features have been introduced to EIPiGraph compared to the previous prototype implementation. The most important are introducing trimmed approximation error with automated determination of the trimming radius and the explicit control for topological complexity. Without these features, elastic principal graphs performed poorly in some applications. A set of grammar operations was redesigned and some application-specific graph rewriting rules were introduced (i.e., for single cell data analysis, extending tree branches and rewiring the branching point). EIPiGraph contains several other novelties such as: a) the ability to approximate complex data by principal graph ensembles, b) the inference of a consensus graph structure from a graph ensemble, c) the ability to manage principal forest-based data approximators, d) and ability to deal with non-tree like data structures.

EIPiGraph is currently implemented in five programming languages (R, Matlab, Python, Scala, Java) which makes it easily applicable in many scientific domains. The R version is accompanied by a graphical user interface allowing the user to interact with the principal graph and make data queries based on its structure.

Results

EIPiGraph correctly recovers complex data topologies in synthetic examples

As a first step in our analysis, we applied EIPiGraph on a synthetic 2D datasets describing a circle connected to branching structure. EIPiGraph was able to easily recover the target structure when the right grammar rules are specified (Figure 2B). We underline that the use of grammars gives EIPiGraph great flexibility in approximating data structures with non-trivial structures. In the simplest case it requires to know *a priori* the type of the topology (e.g., curve, circular, tree-like) of the dataset to approximate. However, as discussed later, EIPiGraph is also able to provide a data approximator when no information is available on the underlying topology of the data.

EIPiGraph is highly robust to noise

We then explored the robustness of EIPiGraph to down and oversampling (Figure 2A). Our algorithm is able to properly recover the structure of the data, regardless of the condition being considered, with only minimal differences in the position of the branching points due to the loss of information associated with downsampling. Then, we tested the robustness of EIPiGraph to Gaussian noise (Figure 2C). As the percentage of noisy points increases, certain features of the data are not captured by the approximator, as expected. However, even in the presence of a striking amount of noise, EIPiGraph is capable of correctly recovering (at least partly) the underlying data distribution. To achieve this remarkable robustness to noise, EIPiGraph employs a trimmed definition of mean squared error, which allows the algorithm to learn the structure of a complex dataset from an appropriately chosen local fragment, and sequentially extending it³². In the examples of Figure 2C, the tree is being constructed starting from the densest part of the data space.

EIPiGraph is capable of disentangling intersecting threads

Disentangling intersecting curvilinear manifolds is a hard to solve problem (sometimes called the Travel Maze problem) that is described in the field of computer vision and other fields³³. The intrinsic rigidity of elastic graph in combination with a trimmed approximation error enables EIPiGraph to solve the Travel Maze problem quite naturally. This is possible because the local version of the elastic graph algorithm is characterized by certain

persistence in choosing the direction of the graph growth. Indeed, when presented with a dataset corresponding to a group of three threads intersecting on the same plane, EIPiGraph is able to recognize them and cluster the data points accordingly to each detected path (Figure 2D).

EIPiGraph can take advantage of the full dimensionality of the data

As demonstrated by the widespread use of tools like PCA, tSNE, LLE, or diffusion maps, dimensionality reduction can be a powerful tool to better visualize the structure of data. However, some data features can be lost as the dimension of the dataset is being reduced. This can be particularly problematic if dimensionality reduction is used as an intermediate step which is part of a long analytical pipeline. To illustrate this phenomenon, we generated a 10-dimensional dataset describing an *a priori* known branching processes. When the points are projected into a 2D plane of first two principal components, one of branches collapses and becomes indistinguishable (Figure 2E). This effect is due to the branch under consideration being essentially orthogonal to the space of first two principal components. As expected, EIPiGraph is unable to capture the collapsed branch, when it is used on the 2D PCA projection of the data. However, the branch is correctly recovered when EIPiGraph is run using all the 10 dimensions.

EIPiGraph allows an explicit control of graph complexity

In many circumstances, it may be important to control the *level of branching* of the data approximator. For example, this is the case if some *a priori* information is available on the data structure or on the level of noise present. To deal with this situation EIPiGraph can be used with the *tuning parameter* α , which allows penalizing the appearance of complex branching points. In particular, if $\alpha=0$ branching is not penalized, while larger values progressively penalize branching, with $\alpha\approx 1$ resulting in branching being completely forbidden (a more formal discussion of α is presented in the Methods section). Supplementary Figure 1 illustrates using the standard iris and a synthetic dataset how changing this parameter eliminates non-essential branches of a fitted principal tree, up to prohibiting them and simplifying the principal tree structure to a simple principal curve. Without this penalty term, extensive branches can appear in the regions of data distributions which can be characterized as “thick turn”, i.e., when the increased local curvature of the intrinsic underlying manifold leads to increased local variance of the dataset (Supplementary Figure 1).

EIPiGraph is able to approximate datasets containing millions of points, without pre-clustering or downsampling

“Big data” containing hundreds of thousands of points with multiple dimensions are quite common nowadays, and manifold learning algorithms should be able to deal with such large datasets in a reasonable amount of time. The core functionalities of EIPiGraph are based on a fast algorithm which allows the method to scale quite well to very large datasets. EIPiGraph.R can also take advantage of multiprocessing to further speed up the computation process when necessary. When run on a single core, EIPiGraph.R is able to reconstruct principal curves and circles in few minutes even if tens of thousands points with tens of dimensions are used (Figure 3A). The construction of principal trees is significantly slower due to the combinatorial nature of the search in the structural space, but remains quite fast (Figure 3A). For comparison the R implementation of DDRTree²⁶ is unable to deal with large datasets in reasonable amount of time (Figure 3C). Notably, most of the existing methods are not directly applicable to datasets having more than few thousands of points, and, hence, require data pre-clustering, downsampling or excessively drastic dimension reduction which leads to coarse-graining of the resulting approximator structure. Multicore execution further improves the speed of the EIPiGraph.R making it able to reconstruct a tree with 60 nodes using more than one million three dimensional points in less than 3 hours with 4 cores (Figure 3B). It is worth noting that multicore principal graph construction requires additional memory management operations and may actually slower down the reconstruction for simpler problems, when compared to single core execution (Supplementary Figure 3).

EIPiGraph can use principal graph ensembles to reconstruct a consensus principal graph

Resampling techniques are often used to determine the significance of the data approximator features obtained from analysis of complex datasets^{34,35}. Thanks to its performance, EIPiGraph can be also used in conjunction with resampling to explore the robustness of the reconstruct principal graph. Figure 1C shows a simple example of data resampling applied to the reconstruction of a principal tree. Resampling produces a *principal graph ensemble*, i.e., a set of k principal graphs produced by random sampling of $p\%$ of data points and applying EIPiGraph k times (in Figure 1C, $k = 100$ and $p = 90\%$). From this example it is possible to judge how a different level of uncertainty is associated with different parts of the tree and to explore the uncertainty associated with a branching point.

In more complex examples principal graph ensemble can be even used to infer a *consensus principal graph*, i.e. a principal graph obtained by combining the information of the graph of the ensemble in such a way to discover emergent complex topological features of the data (see Methods). For example, a consensus principal graph constructed by combining an ensemble of trees may contain loops, which are not present in any of the constructed principal trees (Figure 5).

EIPiGraph can manage disconnected principal graphs

As it was shown in the context of the Travel Maze problem, EIPiGraph is capable of dealing with disconnected graphs. This feature is helpful if the data to be approximated are composed of separated clusters. Under these circumstances, the local version of principal graphs should be used (by setting the trimming radius to a finite value) with appropriated initial conditions. Then, the data points approximated by the graph are removed from the data and the construction of principal graphs is repeated until no points remain associated to a graph. Note that resampling can also be used at any step if necessary.

EIPiGraph can infer branching pseudo-time from single-cell RNASeq data

Thanks to the emergence of single cell RNA Sequencing (scRNA-Seq), it is now possible to measure gene expression levels across thousands to millions of single cells. Using these data, it is then possible to look for *paths in the data* that may be associated with the level of cellular commitment and use the positions of cells along these paths (called *pseudotime*) to explore how gene expression changes as cells increase their level of commitment (Figure 4A). This kind of analysis is a powerful tool that has been used, e.g., to explore the biological changes associated with development¹⁷, cellular differentiation¹⁸⁻²⁰, and cancer biology²¹.

EIPiGraph is being used as part of STREAM³⁶, an integrated analysis tool that provides a set of preprocessing steps and a powerful interface to analyse scRNA-Seq or other single cell data to derive, for example, genes differentially expressed across the reconstructed path. An extensive showcase of the power of EIPiGraph in dealing with biological data as part of the STREAM pipeline is discussed elsewhere³⁶. In the present work, we will limit our analysis to a single case of scRNA-Seq dataset related to haematopoiesis³⁷.

Haematopoiesis is an important biological process that depends on the activity of different progenitors. To better understand this process researchers used scRNA-Seq to sequence cells across 4 different populations³⁷: common myeloid progenitors (CMPs), Granulo-monocyte progenitors (GMPs), Megakaryocyte-erythroid progenitors (MEPs), and dendritic cells (DCs). Using the same preprocessing pipeline used by STREAM, which includes selection of the most variant genes via a LOESS-based method³⁸ and dimensionality reduction by Modified Local Linear Embedding (MLLE)³⁹, we obtained a 3D projection of the original data and applied EIPiGraph with resampling (Figure 4B-E, Supplementary Figure 4).

As Figure 4B-C show, EIPiGraph is able to easily recapitulate the differentiation of CMPs into GMPs and MEPs on the MLLE-transformed data. A further branching point corresponding to early-to-intermediate GMPs into DC can be observed. This differentiation trajectory is characterized by a visible level of uncertainty associated with the branching point. The emerging biological picture is compatible with DC emerging at across a specific, but relatively broad, *range of commitment* of GMPs. However, it is worth noting that the number of DCs present in the dataset under analysis is relatively small (30), and hence that the uncertainty associated with the branching from GMPs to DC may be simply due to the relatively small number of DC sequenced at an early committed state.

It is worth noting that when we used EIPiGraph on the expression matrix restricted to the most variant genes, we could still discover the branching point associated with the differentiation of CMPs into GMPs and MEPs (Supplementary Figure 4). However, DCs do not seem to produce an additional branching, suggesting that MLLE can be a powerful way to discover subtle differences among cell populations.

We can further explore the genetic changes associated to DC differentiation by using the pseudotime value to explore gene expression variation across branches and look for potentially interesting patterns. EIPiGraph.R allows visualizing genes with high variation (Supplementary Figure 4E), high mutual information (Supplementary Figure 4C) when looking at the pseudotime ordering, and significant differences across the diverging branches (Supplementary Figure 4D). Supplementary Figure 4D showcases few genes with interesting dynamics associated with the commitment to DC. Note that in all of the plots, the pseudotime with value .5 corresponds to the DC-associated branching point.

ElPiGraph approximates the large scale-structure of the Universe

Astronomy is a classically data rich discipline, with the data collected by the Danish astronomer Tycho Brahe arguably being one of the first documented examples of scientific Big Data. Nowadays, curated astronomical data catalogues containing extensive information on many features of large and small celestial objects are available to the scientific community to explore the features of the Universe. In particular, the positions of galaxies in the 3D redshift space are likely to provide important information on initial conformation of the Universe⁴⁰.

To explore the potential of ElPiGraph in this domain, we obtained the V8k catalogue, which contains the supergalactic coordinates in the redshift space of 30,124 galaxies with velocities smaller than 8000 km/s⁴⁰. Even by visual inspection, it is quite easy to identify different large scale *filaments* present in the data. The complex distribution of the data clearly limits the application of simple manifold learning techniques that assume a predetermined topology.

As a first step in the analysis of the data, we used 100 resampling trees, with initial starting points randomly placed in the densest region of the data. Then, we removed the points captured by at least 20 of the trees and repeated the procedure until the majority of the points were associated to at least 20 trees. This led to a *bootstrapped principal forest* (Figure 5), which we then used to construct a *set of consensus graphs*. From this analysis, clear non-trivial structures emerge: linear paths, interconnected closed loops, and branching points can be observed in the consensus graphs. This example clearly shows the ability of ElPiGraph to extract structural information even when the expected topology of the data under consideration is unknown or too complex to be described by simple grammars.

Discussion

Bigger, and more complex, data are becoming more and more common across many scientific disciplines and being able to extract the relevant features of these data is an important step in deriving and testing scientific hypotheses. ElPiGraph represents a flexible approach for approximating a cloud of data points in a multidimensional space by reconstructing a one-dimensional continuum passing through the *middle of the data cloud*. This approach is similar to principal curve fitting, but allows significantly more complex topologies with, for example, branching points, self-intersections and closed paths. ElPiGraph is specifically designed to be robust with respect to the noise in the sampling of the underlying manifold and is able to scale up to millions of multidimensional points. These features, together with an explicit control of the structural graph complexity, make ElPiGraph applicable in many scientific domains, from data analysis in molecular biology to image recognition, and even to the analysis of complex astronomical data.

Determining the correct topology of an intrinsic data manifold without strong a priori constraints remains a challenging problem due to the combinatorial complexity of this task. In the case of highly noisy data sample or complex (i.e., self-intersecting) manifold structures, the problem itself can be sometimes even ill-posed. However, even in these circumstances, ElPiGraph is able to extract a *data structure skeleton* which can provide a useful approximation that can be used for data visualization and clustering.

By specifying in advance a space of suitable graph structures and by penalizing excessively complex topologies, graph grammars allow exploiting, in an organized way, only a limited subspace of the combinatorial graph structure space. As such, ElPiGraph explores more exhaustively candidate graph structures during while searching the best structure when compared than competitor methods which usually rely on heuristic approaches in order to define one graph structure for a given cloud of data points.

One of the key problem in finding an intrinsic data manifold topology is the presence of multiple local minima in the optimization criteria. Hence it is very important to define problem-specific ways of guessing a rough approximation of the initial graph structure. Under most circumstances the structure exploration procedure of ElPiGraph is capable to improve the initial guess graph structure that may be too complex, or too coarse-grained. This is achieved by applying an optimal sequence of graph structure simplification, or complexification, rewriting rules. Another important tool available in ElPiGraph to avoid spurious atypical local minima is its ability to apply bootstrapping based on resampling. ElPiGraph is able to employ this approach even for large datasets, due to its highly optimized performance which allows approximating the data by an ensemble of principal graphs and, when necessary, by constructing a consensus principal graph, as we have demonstrated in above.

It is worth stressing that efficient data approximation algorithms do not overcome the need for careful data pre-processing, selection of the most informative features, and filtering of potential artefacts present in the data; since the resulting data manifold topology crucially depend on these steps. The application of ElPiGraph to scRNA-Seq

data describing haematopoiesis clearly exemplifies this aspect, as the application of MLE was able to highlight important features of the data that were otherwise hard to distinguish.

It is worth stressing that the methodological approach employed by elastic principal graphs is not limited to reconstructing intrinsically one-dimensional data manifolds. Similar to self-organizing maps, principal graphs organized into regular grids can effectively approximate data manifolds of relatively low intrinsic dimensions (up to four dimensions in practice due to the exponential increase in the number of nodes). Previously such approach was implemented in the method of elastic maps^{12,14}, which requires introducing non-primitive elastic graphs characterized by several selections of subgraphs (stars) in the elastic energy definition. The method of elastic maps has been currently successfully applied for non-linear data visualization, within multiple domains^{13,41-44}. Conceptually, it remains interesting to consider application of elastic principal graph framework to reconstructing intrinsic data manifolds characterized by varying intrinsic dimension.

Methods

Elastic principal graphs: basic definitions

Let G be a simple undirected graph with a set of vertices V and a set of edges E . Let $|V|$ denote the number of vertices of the graph, and $|E|$ denote the number of edges. Let a k -star in a graph G be a subgraph with $k + 1$ vertices $v_0, v_1, \dots, v_k \in V$ and k edges $\{(v_0, v_i) | i = 1, \dots, k\}$. Let $E^{(i)}(0), E^{(i)}(1)$ denote the two vertices of a graph edge $E^{(i)}$, and $S^{(j)}(0), \dots, S^{(j)}(k)$ denote vertices of a k -star $S^{(j)}$ (where $S^{(j)}(0)$ is the central vertex, to which all other vertices are connected). Let $\text{deg}(v_i)$ denote a function returning the order k of the star with the central vertex v_i and 1 if v_i is a terminal vertex. Let us consider a map $\phi: V \rightarrow \mathbf{R}^m$ which describes an embedding of the graph into a multidimensional space by mapping a node of the graph to a point in the data space. For any k -star of the graph G we call its embedding *harmonic* if the embedding of its central coincides with the mean of the leaf embeddings, i.e. $\phi(\text{central node}) = \frac{1}{k} \sum_{i=1 \dots k} \phi(i)$.

We define an *elastic graph* as a graph with a selection of families of k -stars S_m and for which for all $E^{(i)} \in E$ and $S_m^{(j)} \in S_k$, the corresponding elasticity moduli $\lambda_i > 0$ and $\mu_j > 0$ are defined. *Primitive elastic graph* is an elastic graph in which every non-leaf node (i.e., with a least two neighbors) is associated with a k -star formed by *all* the neighbors of the node. All k -stars in the primitive elastic graph are in the selection, i.e. the S_k sets are completely determined by the graph structure. Non-primitive elastic graphs are not considered here, but they can be used, for example, for constructing 2D and 3D elastic principal manifolds, where a node in the graph can be a center of two 2-stars, in a rectangular grid¹³.

Furthermore, we define an *elastic principal tree* as an acyclic primitive elastic principal graph.

Elastic matrix and elastic energy

For implementations, it is convenient to describe the structure and the elastic properties of the graph by an elastic matrix $EM(G)$. The elastic matrix is a $|V| \times |V|$ symmetric matrix with non-negative elements containing the edge elasticity moduli λ_i at the intersection of rows and lines, corresponding to each pair $E^{(i)}(0), E^{(i)}(1)$, and the star elasticity module μ_j at the diagonal element corresponding to $S^{(j)}(0)$. Therefore, $EM(G)$ can be represented as a sum of two matrices A and M :

$$EM(G) = A(G) + M(G),$$

where A is an analog of the weighted adjacency matrix for the graph G , with elasticity moduli playing the role of weights, and $M(G)$ is a diagonal matrix having non-zero values only for nodes that are centers of stars, in which case the value indicates the elasticity moduli of the star. An example of elastic matrix is shown by Supplementary Figure 2A.

The *elastic energy of the graph embedding* is defined as a sum of squared edge lengths (weighted by the elasticity moduli λ_i) and the sum of squared *deviations from harmonicity* for each star (weighted by the μ_j):

$$U^\phi(G) = U_E^\phi(G) + U_R^\phi(G),$$

$$U_E^\phi(G) = \sum_{E^{(i)}} \left[\lambda_i + \alpha \left(\max \left(2, \text{deg} \left(E^{(i)}(0) \right), \text{deg} \left(E^{(i)}(1) \right) \right) - 2 \right) \left(\phi \left(E^{(i)}(0) \right) - \phi \left(E^{(i)}(1) \right) \right)^2 \right],$$

$$U_R^\phi(G) = \sum_{S^{(j)}} \mu_j \left(\phi(S^{(j)}(0)) - \frac{1}{\deg(S^{(j)}(0))} \sum_{i=1}^{\deg(S^{(j)}(0))} \phi(S^{(j)}(i)) \right)^2.$$

The term describing the deviation from harmonicity in the case of 2-star is a simple surrogate for minimizing the local curvature. In the case of k -stars with $k > 2$ it can be considered as a generalization of local curvature defined for a branching point¹³. Note that $U_R^\phi(G)$ can be re-written as

$$U_R^\phi(G) = \sum_{S^{(j)}} \frac{\mu_j}{\deg(S^{(j)}(0))} \sum_{i=1}^{\deg(S^{(j)}(0))} \left(\phi(S^{(j)}(0)) - \phi(S^{(j)}(i)) \right)^2 - \sum_{S^{(j)}} \frac{\mu_j}{\left(\deg(S^{(j)}(0))\right)^2} \sum_{i=1, p=1, i < p}^{\deg(S^{(j)}(0))} \left(\phi(S^{(j)}(i)) - \phi(S^{(j)}(p)) \right)^2,$$

i.e., the term $U_R^\phi(G)$ can be considered as a sum of the energy of elastic springs connecting the star centers with its neighbors (with elasticity moduli $\mu_j/\deg(S^{(j)})$) and the energy of negative (repulsive) springs connecting all non-central nodes in a star pair-wise (with negative elasticity moduli $-\mu_j/(\deg(S^{(j)}))^2$). The resulting system of springs which energy is minimized is shown in Figure 1A. In simple terms, the elasticity of the principal graph contains three parts: positive springs corresponding to elasticity of graph edges (Figure 1A, Supplementary Figure 2B), negative repulsive springs describing the node repulsion to make the graph embedding function ϕ as smooth as possible (Supplementary Figure 2C), positive springs representing the correction term such that the smoothing would correspond to the deviation of harmonicity (Supplementary Figure 2D).

For implementations, it is convenient to represent the elastic energy in the matrix form, by transforming $EM(G)$ into three auxiliary matrices Λ , Λ^{star_edges} and Λ^{star_leafs} . Λ^{star_edges} is a weighted adjacency matrix for the edges connected to star centers, with elasticity moduli μ_j/k_j , where k_j is the number of edges connected to the j th star center. Λ^{star_leafs} is a weighted adjacency matrix for the negative springs (shown in green in Figure 1A), with elasticity moduli $-\mu_j/(k_j)^2$. Example of transforming the elastic matrix $EM(G)$ into three weighted adjacency matrices Λ , Λ^{star_edges} , Λ^{star_leafs} is shown in Supplementary Figure A-D.

For the system of springs shown in Figure 1A, if one applies a distributed force to the nodes then propagation of the node perturbation will be described by a matrix which is a sum of three graph Laplacians.

$$L(G, EM(G)) = L(\Lambda) + L(\Lambda^{star_edges}) + L(\Lambda^{star_leafs}).$$

We remind that a Laplacian matrix for a weighted adjacency matrix A is computed as

$$L(A)_{ij} = \delta_{ij} \sum_k A_{kj} - A_{ij},$$

where δ_{ij} is the Kroeneker symbol.

Basic optimization algorithm

The basic optimization algorithm fits a graph of a given structure to a finite set of data vectors. We define the optimal embedding of a graph is such a map $\phi: V \rightarrow \mathbf{R}^m$ that minimizes the mean squared distance between the position of graph nodes in and the data points and, at the same time, minimizes the elastic energy of the graph embedment serving a penalty term for the ‘‘irregularity’’ of the graph embedment. The irregularity can be manifested by stretching and non-equal distance between graph node positions (penalized by $U_E^\phi(G)$ and partly by $U_R^\phi(G)$) or by deviation from harmonicity (penalized by $U_R^\phi(G)$).

Assume that we have defined a partitioning K of all data points such that $K(i) = \arg \min_{j=1 \dots |V|} \|X_i - \phi(V_j)\|$ returns an index of a node in the graph which is the closest to the i th data point among all graph nodes. Then our objective function to minimize is

$$U^\phi(X, G) = \frac{1}{\sum w_i} \sum_{j=1}^{|V|} \sum_{K(i)=j} w_i \cdot \min \left(\|X_i - \phi(V_j)\|^2, R_0^2 \right) + U^\phi(G),$$

where w_i is a weight of the data point i (can be unity for all points), $|V|$ is the number of vertices, $\|\cdot\|$ is the usual Euclidean distance and R_0 is a trimming radius that can be used to limit the effect of *points distant from the graph*³².

The objective of the basic optimization algorithm is to find such a map $\phi: V \rightarrow \mathbf{R}^m$ that $U^\phi(X, G) \rightarrow \min$ over all possible elastic graph G embeddings in \mathbf{R}^m . In practice, we are looking for a local minimum of $U^\phi(X, G)$ by applying the expectation-minimization type algorithm, which is described by the pseudo-code below:

ALGORITHM 1: BASE GRAPH OPTIMIZATION FOR A FIXED STRUCTURE OF THE ELASTIC GRAPH

- 1) Initialize the graph G , its elastic matrix $E(G)$ and the map ϕ .
- 2) Compute matrix $L(G, E(G))$.
- 3) Partition the data by proximity to the embedded nodes of the graph (i.e., compute the mapping $K: \{X\} \rightarrow \{V\}$ of a data point i to a graph node j).
- 4) Solve the following system of linear equations to determine the new map ϕ .

$$\sum_{j=1}^{|V|} \left(\frac{\sum_{i:K(i)=j} w_i}{\sum_{i=1}^{|V|} w_i} \delta_{ij} + L(G, EM(G))_{ij} \right) \phi(V_j) = \frac{1}{\sum_{i=1}^{|V|} w_i} \sum_{K(i)=j} w_i X_i,$$

where δ_{ij} is the Kroeneker symbol.

Iterate 3-4 till the map ϕ does not change more than ε in some appropriate measure.

The convergence of the algorithm can be easily proven³² since the $U^\phi(X, G)$ is a Lyapunov function with respect to the Algorithm 1. The base algorithm optimizes the graph embedding ϕ , but contains neither a recipe for initializing the map ϕ , nor a recipe for choosing the structure of the graph G . This initialization can be produced by a number of ways, starting from the structural analysis of the kNN graph after some dimension reduction and/or pre-clustering (e.g., computing a spanning tree) or by other heuristic approaches.

Graph grammar approach for determining the optimal graph topology

In contrast to the majority of existing state-of-the-art methods, EIPiGraph exploits a topological graph grammar-based approach to find an optimal structure, by systematic application of some pre-defined set of graph grammar operations. This allows the algorithm to explore many graph topologies, in the space of all possible graph topologies, using a gradient descent-like algorithm (Figure 1A).

A graph-based data approximator should deal simultaneously with two inter-related aspects: determining the optimal topological structure of the graph and determining the optimal map for embedding this graph topology into the multidimensional space. An exhaustive approach would be to consider all the possible graph topologies (or topologies of a certain class, e.g., all possible trees), find the best mapping of all them into the data space, and select the best one. In practice, due to combinatorial explosion, testing all possible graph topologies is feasible only when a small number of nodes is present in the graph, or under restrictive constraints (e.g., only trivial linear graphs, or assuming a restricted set of topologies with a pre-defined number and types of branching). Determining a globally optimal embedment of a graph with a given topology is usually challenging, because of the energy landscape complexity. This means that in practice one has to use an optimization approach in which both graph topology and the mapping function should be learnt simultaneously.

A graph grammar-based approach for constructing such an algorithm was suggested before^{15 31}. The approach starts from a simple graph G_0 and a simple map $\phi(G_0)$. Then a set of predefined grammar operations which can

transform both the graph topology and the map, is applied starting from a given pair $\{G_i, \phi(G_i)\}$. Each grammar operation Ψ^p produces a set of new graph embeddings possibly taking into account the dataset X :

$$\{\{D^k, \phi(D^k)\}, k = 1 \dots s\} = \Psi^p (\{G_i, \phi(G_i)\}, X).$$

Given a pair $\{G_i, \phi(G_i)\}$ and a set of r different graph operations $\{\Psi^1, \dots, \Psi^r\}$ (which we call a “graph grammar”) and an energy function $\bar{U}^\phi(X, G)$, at each step of the algorithm the energetically optimal candidate graph embedding is selected:

$$\{G_{i+1}, \phi_{i+1}(G_{i+1})\} = \operatorname{argmin}_{\{D^k, \phi(D^k)\}} \left\{ U^{\phi(D^k)}(D^k, X) : \{D^k, \phi(D^k)\} \in \bigcup_{p=1 \dots r} \Psi^p (\{G_i, \phi(G_i)\}, X) \right\}$$

where $\{D^k, \phi(D^k)\}$ is supposed to be optimized (fit to data) after application of a graph grammar, using ALGORITHM 1 with initialization suggested by the graph grammar application (see below).

The pseudocode for this algorithm is provided below:

ALGORITHM 2: GRAPH GRAMMAR BASED OPTIMIZATION OF GRAPH STRUCTURE AND EMBEDMENT

1. Initialize current graph embedding by some graph topology and some initial map $\{G_0, \phi(G_0)\}$.
 2. For the current graph embedding $\{G_i, \phi(G_i)\}$, apply all grammar operations from a grammar $\{\Psi^1, \dots, \Psi^r\}$, and generate a set of s candidate graph embeddings $\{D^k, \phi(D^k), k = 1 \dots s\}$.
 3. Further optimize each candidate graph embedding using ALGORITHM 1, and obtain a set of s energy values $\{\bar{U}^{\phi(D^k)}(D^k)\}$.
 4. Among all candidate graph embeddings, select an embedding with the minimum energy $\{G_{i+1}, \phi_{i+1}(G_{i+1})\}$.
- Repeat 2-4 until the graph contains a required number of nodes.

Note that the energy function $\bar{U}^\phi(X, G)$ used to select the optimal graph structure is not necessarily the same energy as (1-3) and can include various penalties to give less priority to certain graph configurations (such as those having excessive branching as described below). Separating energy functions $U^\phi(X, G)$ used for fitting a fixed graph structure to the data and $\bar{U}^\phi(X, G)$ used to select the most favorable graph configuration allows achieving flexibility in defining the strategy of selecting the most optimal graph topologies.

Simple graph grammar operations

Let us define in details two base grammar operations “bisect an edge” and “add a node to a node”.

<p>GRAPH GRAMMAR OPERATION “BISECT AN EDGE”</p> <p><u>Applicable to:</u> any edge of the graph</p> <p><u>Update of the graph structure:</u> for a given edge {A,B}, connecting nodes A and B, remove {A,B} from the graph, add a new node C, and introduce two new edges {A,C} and {C,B}.</p> <p><u>Update of the elasticity matrix:</u> the elasticity of edges {A,C} and {C,B} equals elasticity of {A,B}.</p> <p><u>Update of the graph embedding:</u> C is placed in the mean position between embeddings of A and B.</p>	<p>GRAPH GRAMMAR OPERATION “ADD NODE TO A NODE”</p> <p><u>Applicable to:</u> any node of the graph</p> <p><u>Update of the graph structure:</u> for a given node A, add a new node C, and introduce a new edge {A,C}</p> <p><u>Update of the elasticity matrix:</u> if A is a leaf node (not a star center) then the elasticity of the edge {A,C} equals to the edge connecting A and its neighbor, the elasticity of the new star with the center in A equals to the elasticity of the star centered in the neighbor of A. If the graph contains only one edge then a predefined values is assigned. else the elasticity of the edge {A,C} is the mean elasticity of all edges in the star with the center in A, the elasticity of a star with the center in A does not change.</p> <p><u>Update of the graph embedding:</u> if A is a leaf node (not a star center) then C is placed at the same distance and the same direction as the edge connecting A and its neighbor, else C is placed in the mean point of all data points for which A is the closest node</p>
---	---

ALGORITHM 2 with a graph grammar containing only ‘bisect an edge’ operation, and initializing the graph by two nodes connected by a single edge, produces an *elastic principal curve*.

ALGORITHM 2 with a graph grammar containing only ‘bisect an edge’ operation, and initializing the graph by four nodes connected by four edges without branching, produces a *closed elastic principal curve* (called elastic principal circle, for simplicity).

ALGORITHM 2 with the growing graph grammar containing both operations ‘bisect an edge’ and ‘add a node to a node’, and initializing the graph by two nodes connected by a single edge produces an *elastic principal tree*. In the case of a tree or other complex graphs, it is advantageous to improve the ALGORITHM 2 by providing an opportunity to ‘roll back’ the changes of the graph structure. This gives an opportunity to get rid of unnecessary branching or to merge split branches created in the history of graph optimization, if this is energetically justified (see Supplementary Figure 2B). This possibility can be achieved by introducing a shrinking grammar. In the case of tree, the shrinking grammar consists of two operations ‘remove a leaf node’ and ‘shrink internal edge’ (defined below). Then the graph growth can be achieved by alternating two steps of application of the growing grammar with one step of application of the shrinking grammar. In each such a cycle, one node will be added to the graph.

<p>GRAPH GRAMMAR OPERATION “REMOVE A LEAF NODE”</p> <p><u>Applicable to:</u> node A of the graph with $\text{deg}(A)=1$</p> <p><u>Update of the graph structure:</u> for a given edge {A,B}, connecting nodes A and B, remove edge {A,B} and node A from the graph</p> <p><u>Update of the elasticity matrix:</u> if B is the center of a 2-star then put zero for the elasticity of the star for B (B becomes a leaf) else do not change the elasticity of the star for B</p> <p>Remove row and column correspond to vertex A</p> <p><u>Update of the graph embedding:</u> all nodes besides A keep their positions.</p>	<p>GRAPH GRAMMAR OPERATION “SHRINK INTERNAL EDGE”</p> <p><u>Applicable to:</u> any edge {A,B} such that $\text{deg}(A)>1$ and $\text{deg}(B)>1$.</p> <p><u>Update of the graph structure:</u> for a given edge {A,B}, connecting nodes A and B, remove {A,B}, reattach all edges connecting A with its neighbours to B, remove A from the graph.</p> <p><u>Update of the elasticity matrix:</u> The elasticity of the new star with the center in B becomes average elasticity of the previously existing stars with the centers in A and B Remove row and column correspond to vertex A</p> <p><u>Update of the graph embedding:</u> B is placed in the mean position between A and B embeddings.</p>
--	--

Note that, when applicable, the above operations, can be restricted so that they are applied only to nodes with a certain ranges of degrees to better explore. This can be helpful, for example, if the applied grammar is designed to better explore the vicinity of a branching point or a leaf node.

Robust local construction of elastic principal graphs

In the form of the EIPiGraph optimization criterion $U^\phi(X, G)$, data points located more distantly than R_0 (a parameter called “trimming radius”) from any graph node position do not contribute, for a given data point partitioning, to the optimization equation in Algorithm 1. However, these data points might appear at the distance smaller than R_0 at the next algorithm iteration: therefore, it is not equivalent to permanent pre-filtering “outliers”. The approach is similar to the “data-driven” trimmed k-means clustering⁴⁵.

The robust version of the algorithm can tolerate significant amount of uniformly distributed background noise (see Figure 2C) and even deal with self-intersecting data distributions (Figure 2D), if the trimming radius is properly chosen. EIPiGraph includes a function for estimating the coarse-grained radius of the data based on local analysis of density distribution, which can be used as a good initial guess for the R_0 value.

In case of existence of several well-separable clusters in the data, with the distance between them larger than R_0 , robust version of EIPiGraph can approximate the principal graph only for one of them, completely disregarding the rest of the data. In this case, the approximated part of the data can be removed and the robust EIPiGraph can be re-applied. For example, this procedure will construct a second (third, fourth, etc.) principal tree. Such an approach will approximate the data by disconnected “principal forest”.

Alternative ways of constructing robust principal graphs include using piece-wise quadratic subquadratic error functions (PQSQ potentials)⁴⁶. It uses computationally efficient non-quadratic error functions for approximating a dataset. These two approaches will be implemented in the future versions of EIPiGraph.


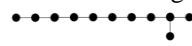

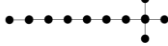
Strategies for graph initialization

The construction of elastic principal graphs in EIPiGraph can be organized either by graph growth (similar to divisive clustering) or by shrinking the graph (similar to agglomerative clustering) or by exploring possible graph structures having the same number of nodes. These different strategies can be achieved by specifying the appropriate graph grammars in the parameter set. Seeding the initial graph structure can have a strong influence on the final graph mapping to the data space and its structure.

Default setting of EIPiGraph initializes the graph with the simplest graph containing two nodes oriented along the first principal component: this initialization is able to correctly fit data topology in relatively simple cases. Other initializations are advised in the case of more complex distributions: for example, applying pre-clustering and computing (once) the minimal spanning tree between cluster centroids can be used for the initialization of the principal tree (e.g., a similar approach is used by the STREAM pipeline³⁶).

When using a finite trimming radius R_0 value, the graph growing can be initialized by 1) a rough estimation of local data density in a limited number of data points and 2) placing two nodes, one into the data point characterized by the highest local density and another node is placed into the data point closest to the first one (but not coinciding).

Control for excessive branching

Principal trees can suffer from excessive branching in the regions of data space where the local effective dimension of data is far from one. In case of EIPiGraph, changing the elasticity parameters, especially λ allows partially control of the excessive branching: however, this changes other properties of the elastic principal graph. EIPiGraph contains a control (α parameter) setting an explicit penalty for the stars of higher order. From several considerations, it appears the most effective to include this penalty within the elastic stretching part $U_E^\phi(G)$ of the elastic energy. Let us consider graph structures each having 11 nodes and 10 edges of equal unity length. Then, for example,  graph is characterized by $U_E^\phi(G) = 10\lambda$ contribution to the elastic energy. Graph with one star  will be characterized by $U_E^\phi(G) = 10\lambda + 3\alpha$ penalty,  by $U_E^\phi(G) = 10\lambda + 6\alpha$,  by $U_E^\phi(G) = 10\lambda + 8\alpha$.

In case of presence of excessive branching, it is recommended to set up the first branching control parameter α to a small value (e.g., 0.01). Changing the value of α from 0 to a large value (e.g., 1) allows gradual change from the absence of excessive branching penalty to effective interdiction of branching (thus, constructing a principal curve instead of a tree as a result, see Supplementary Figure 1). In Supplementary Figure 1, an example of application of the penalty α is shown using a simple example of a data distribution characterized by a “think turn” area.

Implementations of the algorithm

The EIPiGraph method is implemented in several programming languages:

R and MATLAB implementations are available from <https://github.com/sysbio-curie/EIPiGraph.R> and <https://github.com/sysbio-curie/EIPiGraph.M> correspondingly.

Java implementation of EIPiGraph makes a part of VDAOEngine library (<https://github.com/auranic/VDAOEngine/>) for high-dimensional data analysis developed by Andrei Zinovyev. Developing Java code for EIPiGraph is not an active effort anymore, and implementation of EIPiGraph in Java does not scale as good as other implementations.

Python implementation is available at <https://github.com/AlexiMartin/EIPiGraph.P>

Scala implementation is available from <https://github.com/mraad/elastic-graph>.

All implementations contain the core algorithm code described in this document. However, implementations differ in the set of functionalities improving the core algorithm such as robust local version of the algorithm, boosting up the algorithm performance by local optimization of candidate graphs, using the resulting graphs in various applications.

Acknowledgements

This work is supported by Ministry of Education and Science of Russia (Project No. 14.Y26.31.0022), by ITMO Cancer SysBio program (MOSAIC) and INCa PLBIO program (CALYS, INCA_11692).

References

1. Gorban, A. N. & Yablonsky, G. S. Grasping Complexity. *Comput. Math. with Appl.* **65**, 1421–1426 (2013).
2. Zinovyev, A. Overcoming Complexity of Biological Systems: from Data Analysis to Mathematical Modeling. *Math. Model. Nat. Phenom.* **10**, 186–205 (2015).
3. Rayón, P. & Gromov, M. Isoperimetry of waists and concentration of maps. *Geom. Funct. Anal.* **13**, 178–215 (2003).
4. Gorban, A. N. & Tyukin, I. Y. Stochastic separation theorems. *Neural Networks* **94**, 255–259 (2017).
5. Gorban, A. N. & Tyukin, I. Y. Blessing of dimensionality: mathematical foundations of the statistical physics of data. *Philos. Trans. R. Soc. A Math. Phys. Eng. Sci.* **376**, (2018).
6. Pearson, K. 1901. On lines and planes of closest fit to systems of points in space. 559–572 (1901).
7. Kohonen, T. The self-organizing map. *Proc. IEEE* **78**, 1464–1480 (1990).
8. Tenenbaum, J. B., De Silva, V. & Langford, J. C. A global geometric framework for nonlinear dimensionality reduction. *Science (80-.)*. **290**, 2319–2323 (2000).
9. Roweis, S. T. & Saul, L. K. Nonlinear dimensionality reduction by locally linear embedding. *Science (80-.)*. **290**, 2323–2326 (2000).
10. Van Der Maaten, L. J. P. & Hinton, G. E. Visualizing high-dimensional data using t-sne. *J. Mach. Learn. Res.* **9**, 2579–2605 (2008).
11. Smola, A. J., Williamson, R. C., Mika, S. & Sch, B. Regularized Principal Manifolds. 214–229 (1999).
12. Gorban, A. & Zinovyev, A. Elastic principal graphs and manifolds and their practical applications. *Computing (Vienna/New York)* **75**, 359–379 (2005).
13. Gorban, A. N. & Zinovyev, A. Principal manifolds and graphs in practice: from molecular biology to dynamical systems. *Int. J. Neural Syst.* **20**, 219–232 (2010).
14. Gorban, A., Kégl, B., Wunch, D. & Zinovyev, A. Principal Manifolds for Data Visualisation and Dimension Reduction. *Lect. notes Comput. Sci. Eng.* 340 (2008). doi:10.1007/978-3-540-73750-6
15. Gorban, A. N. & Zinovyev, A. Y. in *Handbook of Research on Machine Learning Applications and*

- Trends: Algorithms, Methods and Techniques* (2008). doi:10.4018/978-1-60566-766-9
16. Zinovyev, A. & Mirkes, E. Data complexity measured by principal graphs. *arXiv12125841* (2012). doi:10.1016/j.camwa.2012.12.009
 17. Furlan, A. *et al.* Multipotent peripheral glial cells generate neuroendocrine cells of the adrenal medulla. *Science* (80-). **357**, (2017).
 18. Trapnel, C. *et al.* Pseudo-temporal ordering of individual cells reveals dynamics and regulators of cell fate decisions. *Nat Biotechnol* **29**, 997–1003 (2012).
 19. Athanasiadis, E. I. *et al.* Single-cell RNA-sequencing uncovers transcriptional states and fate decisions in haematopoiesis. *Nat. Commun.* **8**, 2045 (2017).
 20. Velten, L. *et al.* Human haematopoietic stem cell lineage commitment is a continuous process. *Nat. Cell Biol.* **19**, 271–281 (2017).
 21. Tirosh, I. *et al.* Single-cell RNA-seq supports a developmental hierarchy in human oligodendroglioma. *Nature* **539**, 309–313 (2016).
 22. Cannoodt, R., Saelens, W. & Saeys, Y. Computational methods for trajectory inference from single-cell transcriptomics. *European Journal of Immunology* **46**, 2496–2506 (2016).
 23. Moon, K. R. *et al.* Manifold learning-based methods for analyzing single-cell RNA-sequencing data. *Curr. Opin. Syst. Biol.* (2017). doi:10.1016/j.coisb.2017.12.008
 24. Saelens, W. *et al.* A comparison of single-cell trajectory inference methods: towards more accurate and robust tools. *bioRxiv* 276907 (2018). doi:10.1101/276907
 25. Drier, Y., Sheffer, M. & Domany, E. Pathway-based personalized analysis of cancer. *Proc. Natl. Acad. Sci.* **110**, 6388–6393 (2013).
 26. Qiu, X. *et al.* Reversed graph embedding resolves complex single-cell trajectories. *Nat. Methods* (2017). doi:10.1038/nmeth.4402
 27. Welch, J. D., Hartemink, A. J. & Prins, J. F. SLICER: Inferring branched, nonlinear cellular trajectories from single cell RNA-seq data. *Genome Biol.* **17**, (2016).
 28. Setty, M. *et al.* Wishbone identifies bifurcating developmental trajectories from single-cell data. *Nat. Biotechnol.* **34**, 637–645 (2016).
 29. Kégl, B. & Krzyzak, A. Piecewise linear skeletonization using principal curves. *IEEE Trans. Pattern Anal. Mach. Intell.* **24**, 59–74 (2002).
 30. Gorban, A. N., Sumner, N. R. & Zinovyev, A. Y. Beyond the concept of manifolds: principal trees, metro maps, and elastic cubic complexes. in *Lecture Notes in Computational Science and Engineering* **58**, 219–237 (2008).
 31. Gorban, A. N., Sumner, N. R. & Zinovyev, A. Y. Topological grammars for data approximation. *Appl. Math. Lett.* **20**, 382–386 (2007).
 32. Gorban, A. N., Mirkes, E. & Zinovyev, A. Y. Robust principal graphs for data approximation. *Arch. Data Sci.* **2**, 1:16 (2017).
 33. Babaeian, A., Bayestehtashk, A. & Bandarabadi, M. Multiple manifold clustering using curvature constrained path. *PLoS One* **10**, (2015).
 34. Politis, D., Romano, J. & Wolf, M. *Subsampling*. (Springer, 1999).
 35. Albergante, L., Blow, J. J. & Newman, T. J. Buffered Qualitative Stability explains the robustness and evolvability of transcriptional networks. *Elife* **3**, e02863 (2014).
 36. Chen, H. *et al.* STREAM: Single-cell Trajectories Reconstruction, Exploration And Mapping of omics data. *bioRxiv* 302554 (2018).
 37. Paul, F. *et al.* Transcriptional Heterogeneity and Lineage Commitment in Myeloid Progenitors. *Cell* **163**, 1663–1677 (2015).
 38. Guo, G. *et al.* Serum-Based Culture Conditions Provoke Gene Expression Variability in Mouse Embryonic Stem Cells as Revealed by Single-Cell Analysis. *Cell Rep.* **14**, 956–965 (2016).
 39. Zhang, Z. & Wang, J. MLLE: Modified Locally Linear Embedding Using Multiple Weights. *Adv. Neural Inf. Process. Syst.* 1593–1600 (2006).
 40. Courtois, H. M., Pomarède, D., Tully, R. B., Hoffman, Y. & Courtois, D. Cosmography of the local universe. *Astron. J.* **146**, (2013).
 41. Gorban, A. N. & Zinovyev, A. Visualization of data by method of elastic maps and its applications in genomics, economics and sociology. *IHES Prepr.* (2001).
 42. Gorban, A. N., Zinovyev, A. Y. & Wunsch, D. C. Application of the method of elastic maps in analysis of genetic texts. *Proc. Int. Jt. Conf. Neural Networks, 2003.* **3**, (2003).
 43. Failmezger, H., Jaegle, B., Schrader, A., Hülskamp, M. & Tresch, A. Semi-automated 3D Leaf Reconstruction and Analysis of Trichome Patterning from Light Microscopic Images. *PLoS Comput. Biol.* **9**, (2013).
 44. Cohen, D. P. A. *et al.* Mathematical Modelling of Molecular Pathways Enabling Tumour Cell Invasion and Migration. *PLOS Comput. Biol.* **11**, e1004571 (2015).

45. Cuesta-Albertos, J. A., Gordaliza, A. & Matrán, C. Trimmed k-means: An attempt to robustify quantizers. *Ann. Stat.* **25**, 553–576 (1997).
46. Gorban, A. N., Mirkes, E. M. & Zinovyev, A. Piece-wise quadratic approximations of arbitrary error functions for fast and robust machine learning. *Neural Networks* **84**, 28–38 (2016).

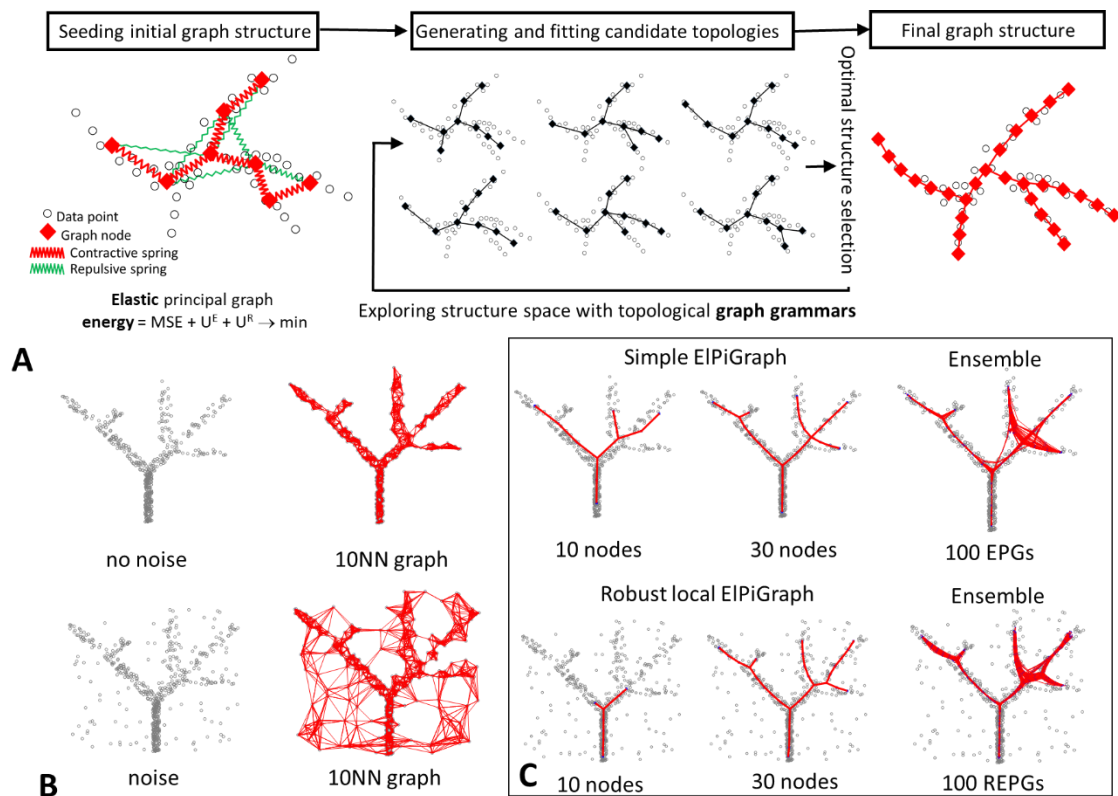


Figure 1. Basic principles and examples of EIPiGraph usage. (A) Schematic workflow of the EIPiGraph method. Left, construction of the elastic graph starts by defining the initial graph topology and embedding it into the data space. The graph structure is fit to the data, using minimization of the mean square error regularized by the elastic energy. The elastic energy includes a term reflecting the overall stretching of the graph (symbolically shown as contractive red springs) and a term reflecting the overall bending of the graph branches and the harmonicity of branching points (shown as repulsive green springs). Middle, EIPiGraph explores a large region of the structural space by exhaustively applying a set of graph rewriting rules (graph grammars) and selecting, at each step, the structure leading to the minimum overall energy of the graph embedding. (B) The structure of the k NN graph used in many manifold learning methods can be misleading in the case of high dimensional data, when data are sampled with noise from a generating manifold, or when background noise is present, as illustrated here. (C) Left and middle, illustration of the robust local workflow of EIPiGraph, which makes it able to deal with the presence of noise. In the global version, the graph structure is fit to all data points at the same time, while in the local version, the structure is fit to the points in the local graph neighbourhood, which expands when the graph grows. Right, an illustration of principal graph ensemble approach: 100 elastic principle graphs are superimposed, each constructed on a fraction of data points randomly sampled at each execution.

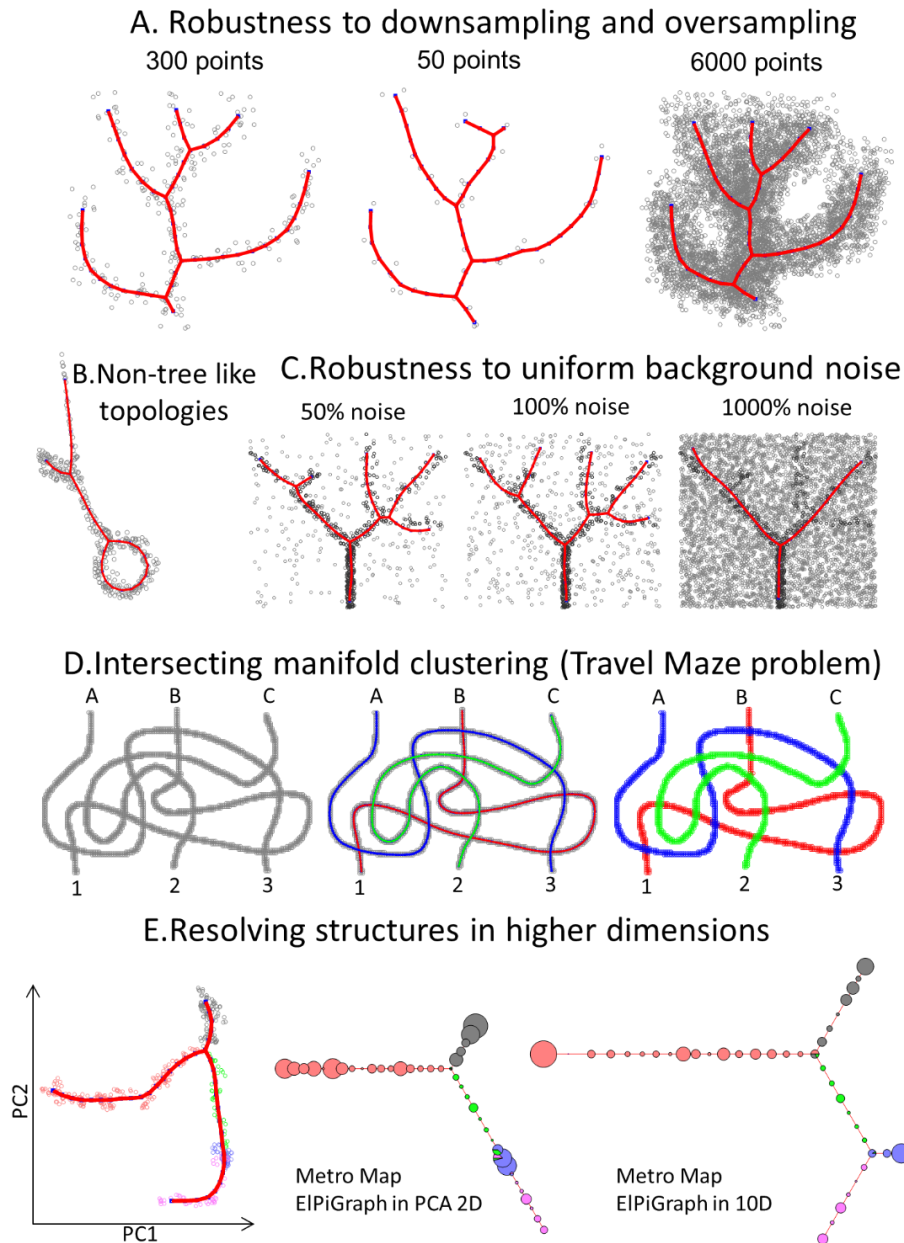


Figure 2. Toy examples showing features of EIPiGraph. (A) EIPiGraph is robust with respect to downsampling and oversampling of a dataset. Here, a reference branching dataset²⁶ is downsampled to 50 points (middle) or oversampled by sampling 20 points randomly placed around each point of the original dataset. (B) EIPiGraph is able to capture non-tree like topologies. Here, the standard set of principal tree graph grammars was applied to a graph initialized by four nodes connected to a ring. (C) EIPiGraph is robust to large amounts of uniformly distributed background noise. Here, the initial dataset from Figure 1 is shown as black points, and the uniformly distributed noisy points are shown as grey points. EIPiGraph is blindly applied to the union of black and grey points. (D) EIPiGraph is able to solve the problem of learning intersecting manifolds. On the left, a toy dataset of three uniformly sampled curves intersecting in many points is shown. EIPiGraph starts by learning a principal curve using the local version several times, each time on a complete dataset. However, each time EIPiGraph is initialized by a pair of neighbouring points not belonging to the points through which a principal curve has already passed through. The extracted curves are shown in the middle by using different colors, and the clustering of the dataset based on curve approximation is shown on the right. (E) Approximating a synthetic ten-dimensional dataset with known branch structure (with different color indicating different branches), where one of the branches (blue one) extrude into higher dimensions and collapses with other branches when projected in 2D by principal component analysis (left). Middle, being applied in the space of two first principal components, EIPiGraph does not recover the branch, while it is captured when the EIPiGraph is applied in the complete ten-dimensional dataset (right). In both cases the principal tree is visualized using metro map layout³⁰.

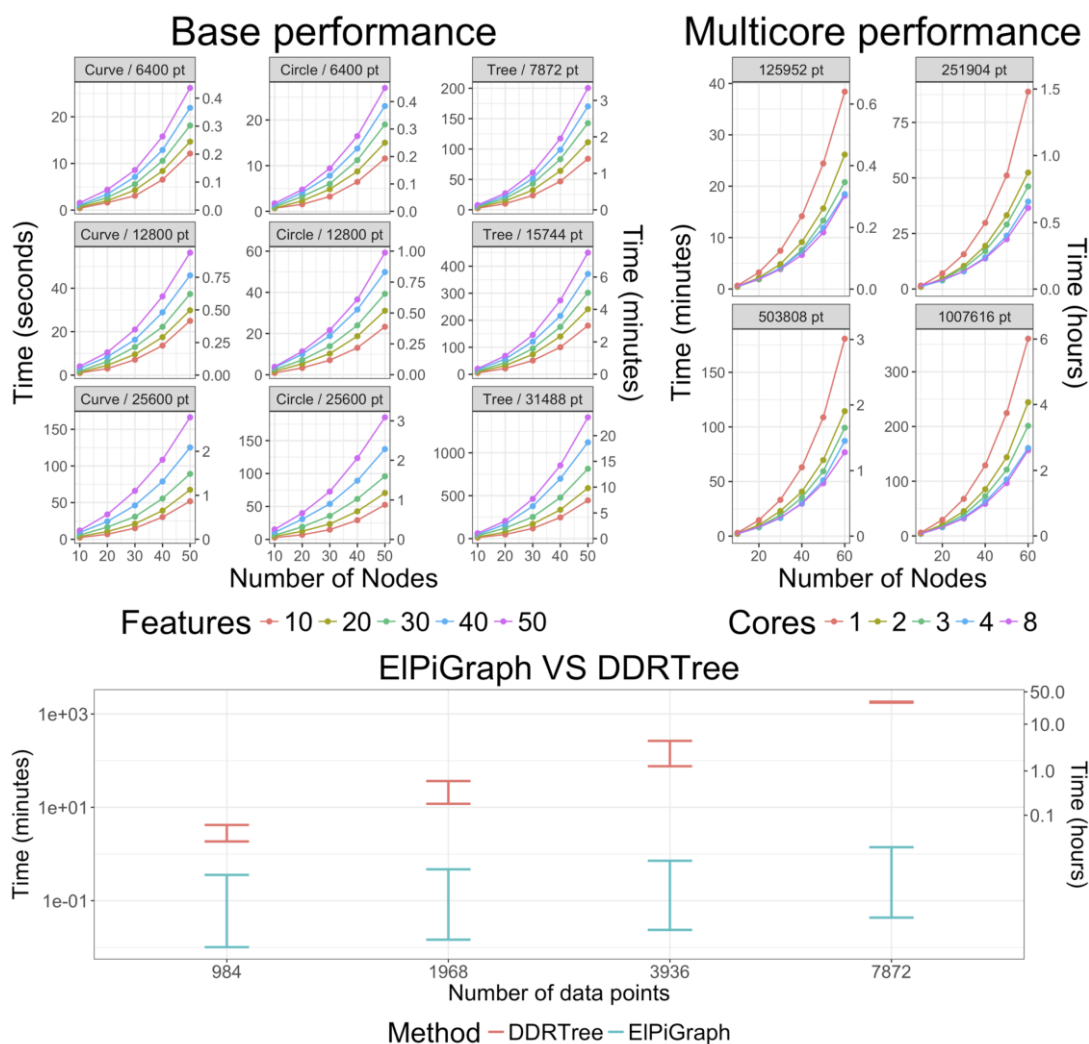


Figure 3. Computational performance of EIPiGraph.R. (A) Time required to build principal curves, circles, and trees (y axis) with a different number of nodes (x axis) using the default parameters across synthetic datasets containing different numbers of points (facets) having a different number of dimensions (color scale) without parallelization. (B) Time required to build principal trees (y axis) with different number of nodes (x axis) using the default parameters across synthetic datasets containing different numbers of three-dimensional points (facets) and a different number of parallel processes (color scale). (D) Time required to perform the DDRTree (y axis) versus the time required to build principal trees using 10-dimensional datasets with a different number of points. For DDRTree, the bar was obtained by selecting between 2 and 10 output dimensions and selecting the slower and faster execution. For EIPiGraph.R, the distribution was obtained by selecting between 10 and 50 nodes using the default parameters. All the tests were run on a CentOS 7 64bit workstation with 16GB of RAM and an Intel Xeon X5472 processor with 8 cores running at 3.00GHz.

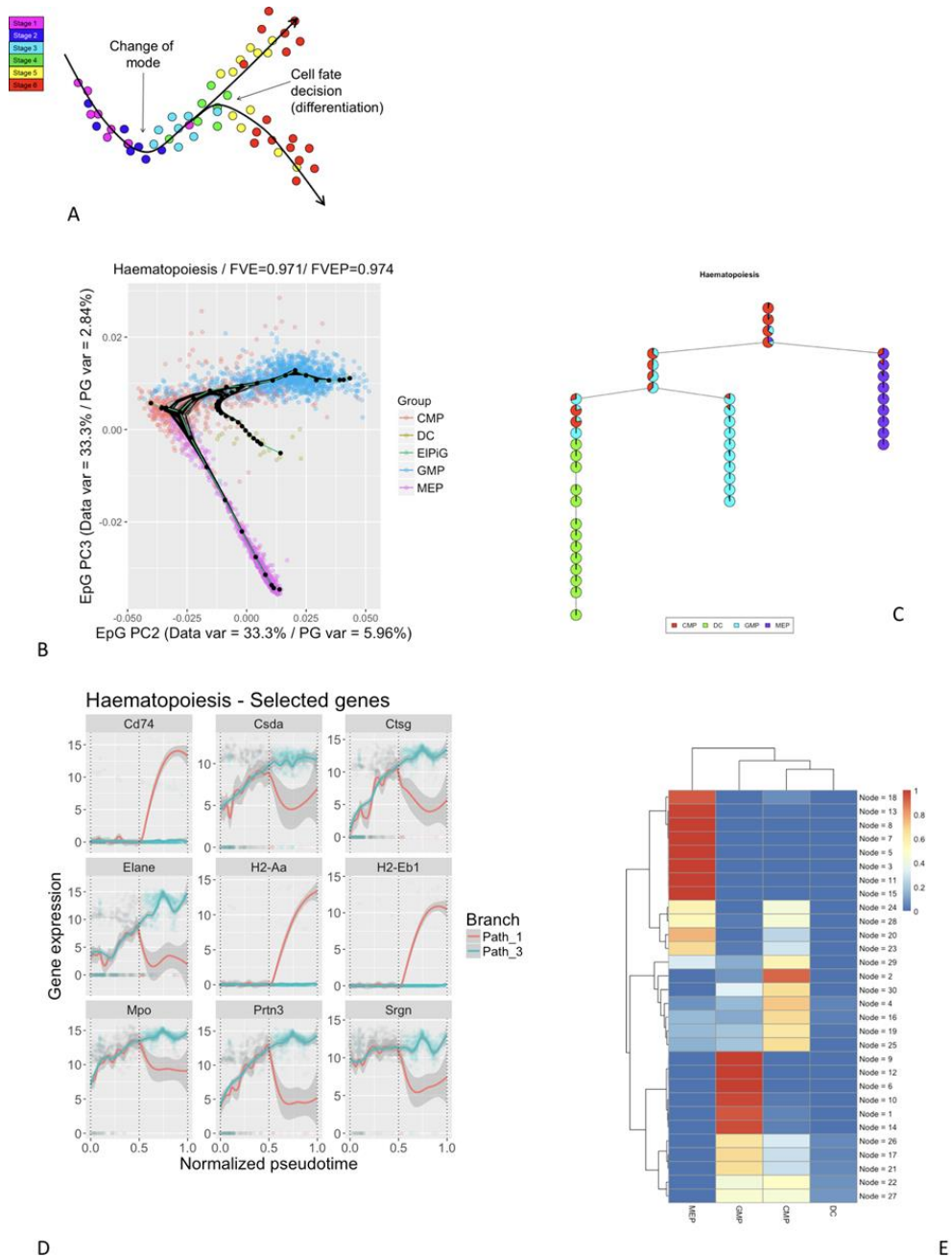


Figure 4. EIPiGraph as a tool to quantify biological pseudotime from single cell data. (A) Diagrammatic representation of the concept behind biological pseudotime in an arbitrary 2D space associated with gene expression: as cells progress from Stage 1 they differentiate (Stage 2 and 3) and branch (Stage 4) into two different subpopulations (Stage 4 and 5). Local distances between the cells indicate genetic similarity. Note how embedding a tree into the data allow recovering genetic changes associated with cell progression into the two differentiated states. (B) Application of EIPiGraph to the scRNA-Seq data³⁷. Each point indicates a cell and is color-coded using the cellular phenotype inferred by the source paper. One hundred bootstrapped trees are represented (in black), along with the single trees (black nodes and green edges). The 2D projection has been obtained by selecting the EIPiGraph principal components 2 and 3. The percentage of variance explained by the projections on the two dimensions of the data (Data var) and nodes of the tree (PG var) are reported along with the fraction of variance of the original data explained by the projection on the nodes (FVE) and on the edges (FVEP). (C) Diagrammatic representation of the distribution of cells across the branches of the tree reconstructed by EIPiGraph. (D) Variation of gene expression along the path from the root of the tree (on the left on panel A) to the branch corresponding to DC commitment (Path_1) and GMP commitment (Path_3). (E) Heatmap showing the ratio of points of different cellular population associated with different nodes.

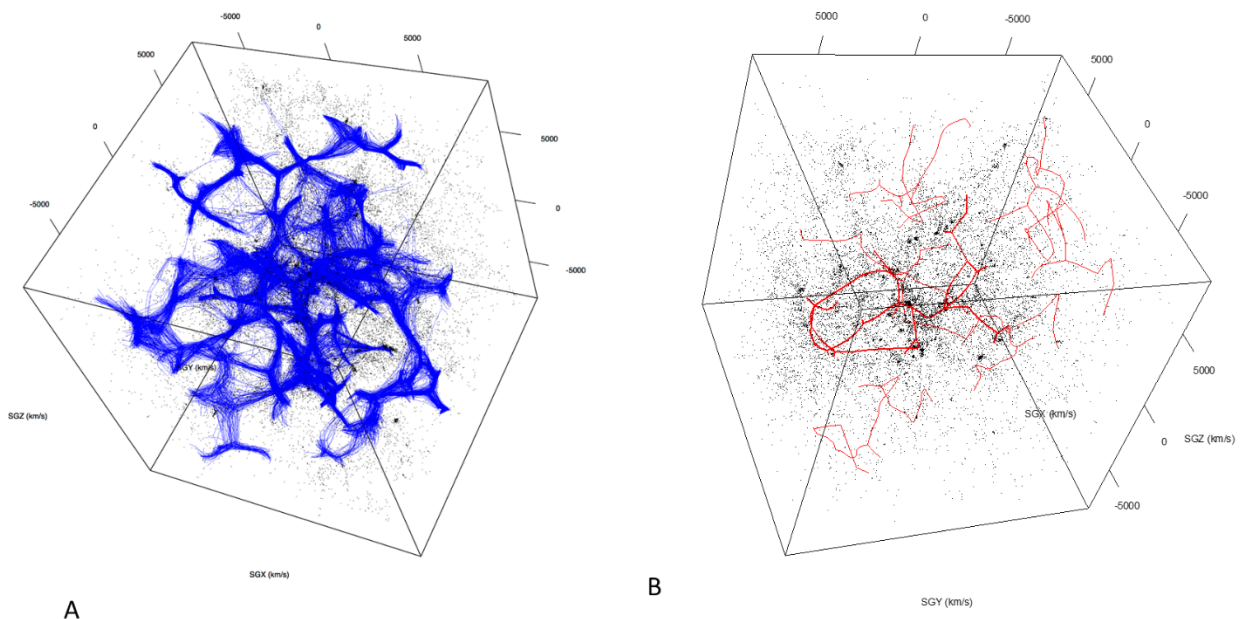
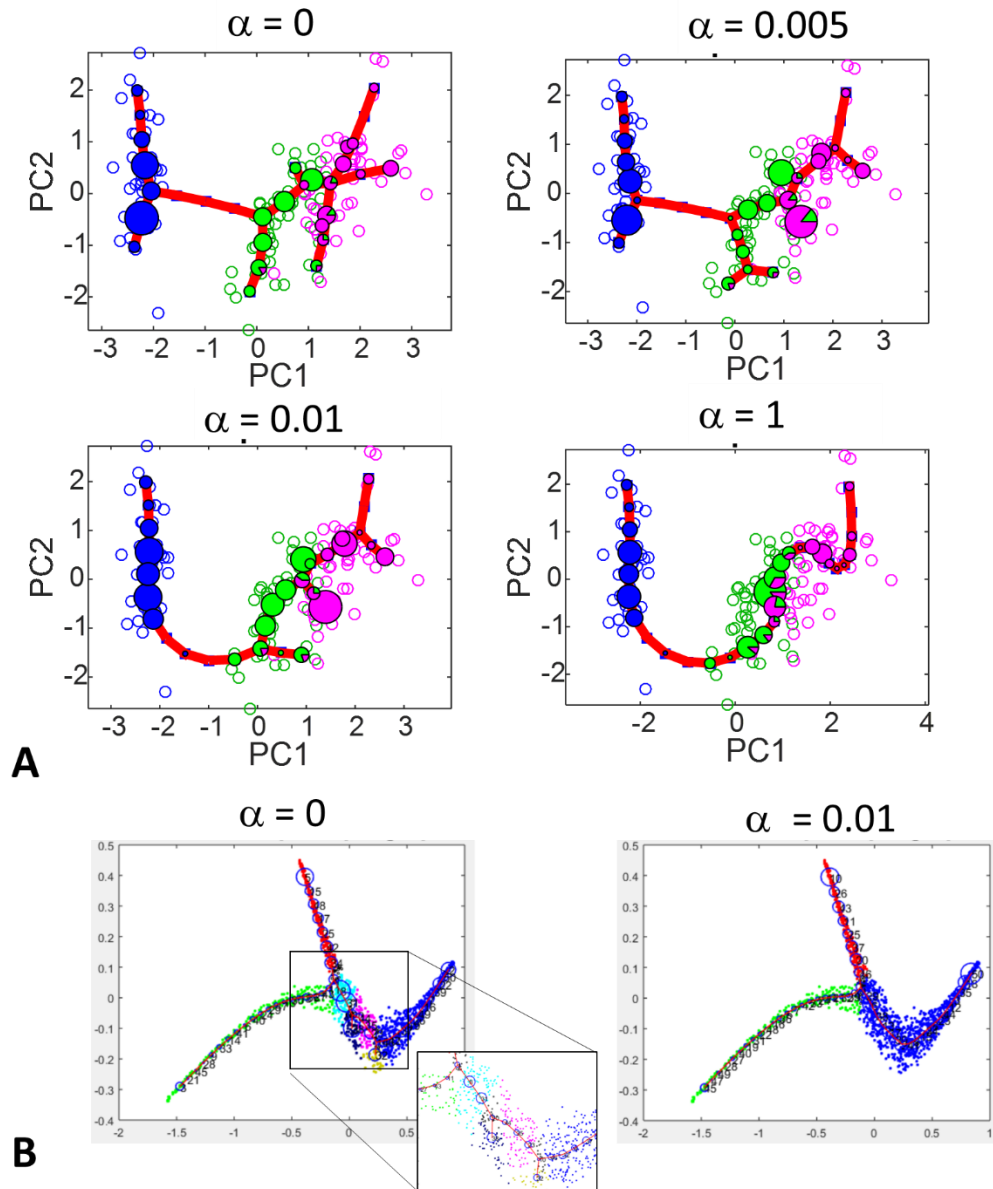


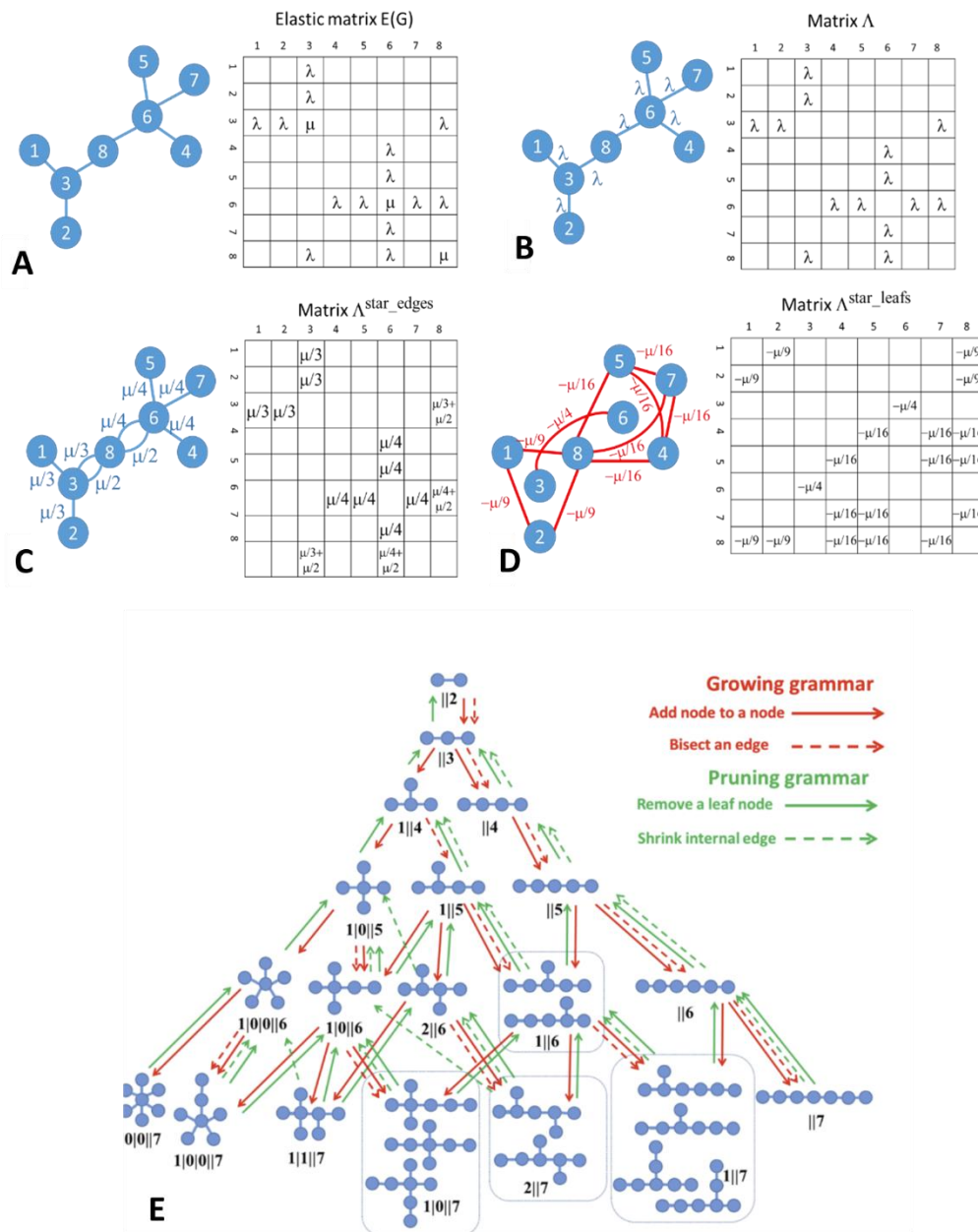
Figure 5. EIPiGraph as a tool to explore complex astronomical data. (A) A bootstrapped principal forest (blue lines) constructed on the V8k catalogue. **(B)** The disconnected consensus graph (red lines) obtained from the bootstrapped principal forest presented by panel A. In both panels, points represent galaxies the axes indicate cartesian components of the velocity in the redshift space.

APPENDIX

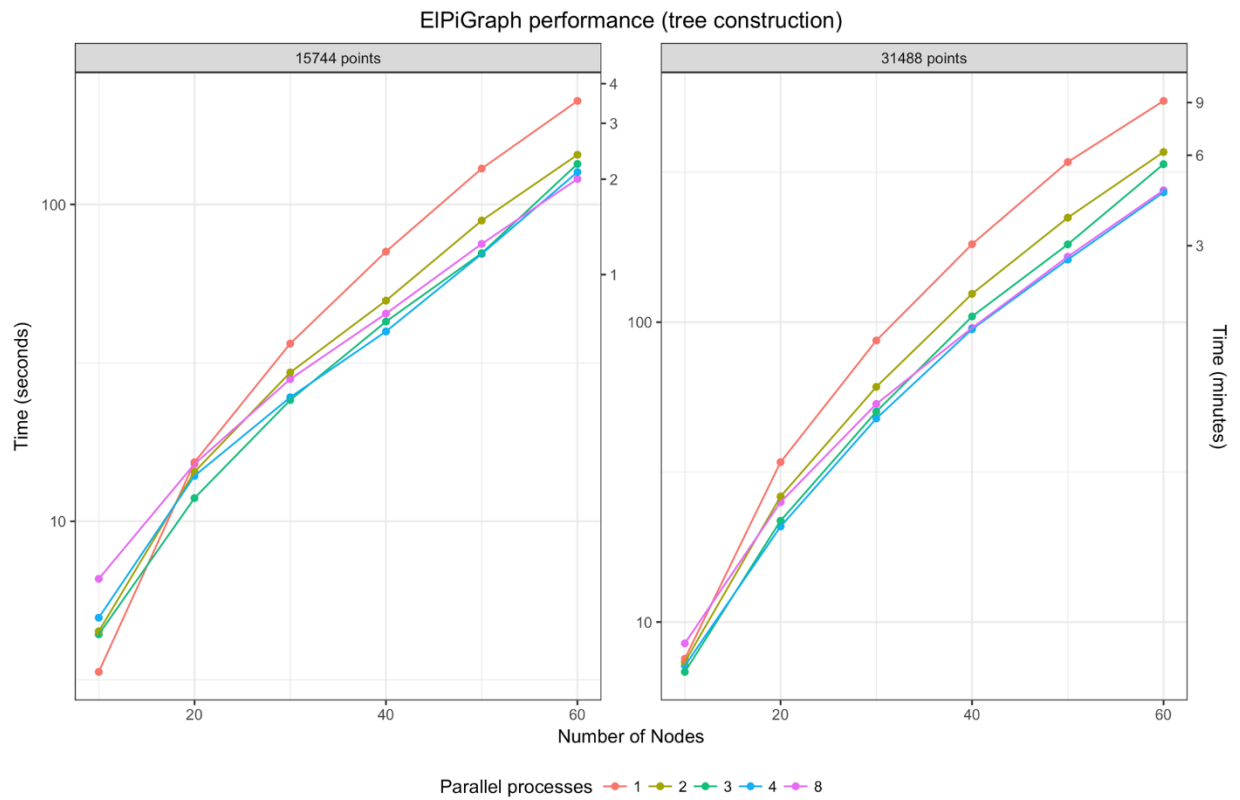


Supplementary Figure 1. Explicit control for topological complexity in EIPiGraph, using α parameter.

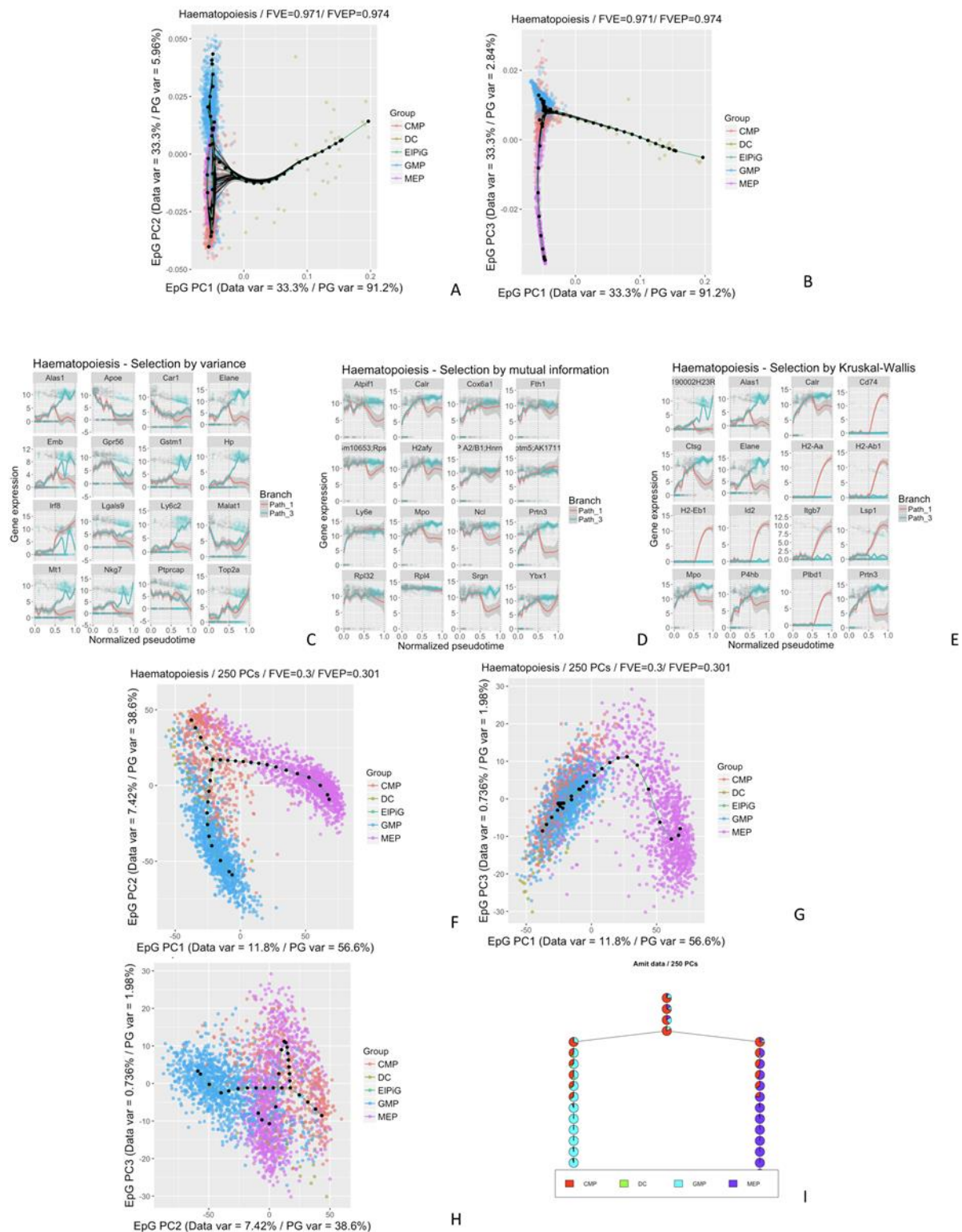
(A) Iris dataset, approximated by EIPiGraph with default parameters, using increasing values of α . (B) Synthetic dataset characterized by a “thick turn” pattern (when the local variance of the dataset increases in the region characterized by the largest curvature of the principal curve). Using explicit control for topological complexity, it is possible to suppress the small branches while retaining the major one. Small fictitious branches appear here due to effective increase of local data dimension, which does not change the data topology.



Supplementary Figure 2. Elastic matrix-based definition of graph elastic energy and searching for the optimal graph topology in the structure space. (A-D) The elastic matrix has dimension $N \times N$, where N is the number of graph nodes (8 in this case). The stretching elasticity moduli λ appear at the intersection of rows and columns, corresponding to each edge (weighted adjacency matrix, shown in panel B). The bending elasticity moduli μ appear at the diagonal elements of the matrix corresponding to the centers of graph k -stars. Bending elastic energy of the graph is described by two weighted adjacency matrices: with positive weights, where each edge receives a weight μ/k from each k -star to which it belongs (panel C) and with negative weights corresponding to all possible pairwise connections between the leaves of each k -star, with weights $-\mu/k^2$ (panel D). (E) All the possible distinct tree-like topologies are shown for graphs with a number of nodes between 1 and 7. Each arrow illustrates the application of a graph rewriting rule (graph grammar operations). A rule can increase the number of nodes (growing, shown in red) or decrease the number of nodes (pruning, shown in green). EIPiGraph explores the space of structures starting from an initial node on this graph and following a trajectory determined by the local increase of the elastic energy of the graph embedding into the data space. In the standard strategy, two growing operations are followed by one pruning operation, in order to avoid an irreversible trapping into a suboptimal graph structure.



Supplementary Figure 3. Reconstruction of a principal tree on 3D datasets with ~15k points and ~31K points and different number of parallel processes.



Supplementary Figure 4. (A-B) Projection of the hematopoietic data discussed in the main text and the principal trees constructed over them in to the 1st and 2nd and 1st and 3rd EIPiGraph principal components with the same graphical conventions of figure 4B. (C-E) Pseudotime-associated dynamics of genes selected using different criteria with the same convections of Figure 4D. (F-H) Projection of the hematopoietic data discussed in the main text without the application of MLLE and the principal trees constructed over them using the principal components derived from the data with the same graphical conventions of figure 4B. (I) Diagrammatic representation of the distribution of cells across the branches of the tree reconstructed by EIPiGraph on the non-MLLE transformed data.